Pramāṇa, Vol. 24, No. 6, June 1985, pp. 825–835. © Printed in India.

A high pressure-high temperature cell for electrical resistivity studies

MOHAMMAD YOUSUF, P Ch SAHU and K GOVINDA RAJAN
Reactor Research Centre, Kalpakkam 603 102, India

MS received 26 July 1984; revised 16 February 1985

Abstract. A high pressure-high temperature cell which permits *in-situ* pressure and temperature calibration is described. The cell is in an opposed anvil configuration, and houses two samples with four probes each along with a miniature furnace and a thermocouple. The pressure and temperature capability of the cell are 100 kbar and 1000°C respectively. This cell was developed to study the electrical resistivity of metals and alloys at high pressure and high temperature. Bismuth was used to calibrate the cell. We report in this paper the design details and the performance of this cell. Ni has been chosen as a test problem and the observed behaviour is indicated to show the quality of data.

Keywords. High pressure-high temperature cell; electrical resistivity; press calibration; bismuth phase diagram.

PACS No. 07·20; 07·35

1. Introduction

For solid state studies under high pressure, the opposed anvil technique is the simplest and the most versatile (Mohammad Yousuf and Govinda Rajan 1982). Introduction of heating adds complications and therefore compatible designs were developed. Multianvil apparatus (Hall *et al* 1963; Hall 1958; Bundy 1962) are novel designs where pressures above 100 kbar and temperature beyond 2000°C have been achieved. For large sample volume, a combination of opposed anvils and a pressure plate—known as 'the belt apparatus' (Hall *et al* 1963; Hall 1956; Daniels and Jones 1961; Hall 1960) was developed. This apparatus has been successfully used to synthesize diamond (Bovenkerk *et al* 1959), cubic boron nitride (Wentorf 1957), stishovite (Coes 1953), etc.

For physical investigations, a simpler set-up which can be handled with ease is called for. Nishikawa and Akimoto (1971) and Ringwood and Major (1968) have developed such simple pressure generating devices for high pressure-high temperature phase diagram studies and to synthesize materials of geological interest. Nishikawa and Akimoto (1971) used the resistivity change in bismuth for pressure calibration and assumed the room temperature calibration data tc be true at high temperature also. Their cell was not adapted for any electrical resistivity measurements. In fact their objective was to subject materials of interest to static pressure of 150 kbar and temperatures above 1000°C and perform x-ray diffraction studies on the product. Our objectives are (i) develop a 2-sample, 8-lead electrical resistivity set-up with the capability of containing hp-ht for sufficiently long duration; (ii) accurately characterise the hp-ht cell *in situ* to generate quantitative data; and (iii) use these data for understanding the physics of solids at high pressures and temperatures.

2. Apparatus and methods

The experimental arrangement is shown in figure 1. An electrically powered hydraulic pump is used to apply the load and heating is accomplished with a high power transformer. *In situ* pressure measurement is done by placing the calibrant such as bismuth, tin, lead inside the sample assembly. The sample temperature is monitored by a thermocouple placed close to the sample. Two constant current sources serve the sample and the calibrant respectively. Four probe resistivity measurements are performed to avoid contact resistance problems inherent in two probe measurements.

The hp-ht electrical resistivity cell is depicted in figure 2. The cell consists of an internally heated graphite furnace. As can be noticed from the figure, the sample and calibrant are almost completely enclosed by the graphite furnace. This arrangement ensures: (i) an almost uniform temperature distribution inside the furnace; (ii) less than 5 min time for the temperature to attain a steady-state; and (iii) good mechanical stability and heat transfer. The temperature distribution was checked by placing 3 thermocouples distributed inside the graphite furnace, as shown in figure 3. Under steady-state conditions, the maximum difference in temperature read by the thermocouples was less than 5°C, indicating a temperature gradient ~ 2°C/mm inside the cell. With the graphite furnace placed inside the cell, it takes less than 5 min for the temperature to reach the highest value set by the dimmerstat marker (see figure 4). The uniform temperature inside the graphite furnace ensures local thermal equilibrium to be achieved. The temperature setting was done manually and maximum difference in successive steps was maintained at about 30°C. This leads to a small rate of increase of temperature ($dT/dt < 15$°C/min). Hence mechanical stability is established avoiding any bursting or shattering of the hp-ht cell. Opposed anvils were used as electrodes to carry the heating current. Here, two effects are noteworthy—if the contact area between the anvil and the graphite furnace is small, the possibility of getting a local hot spot is very high, and this will not only render the anvils very weak, but also reduce the sample pressure very sharply. If the contact area is increased, resistance of the graphite furnace decreases, resulting in utilization of smaller power. The contact area has thus to be optimised. A graphite ring measuring ϕ 12 mm OD, ϕ 9 mm ID with pyrophyllite disc as shown in figure 2 for parts 3 and 4 was found to work satisfactorily for temperatures up to 1000°C.

The following difficulties arise in a set-up like ours, namely,

(i) The electrical leads used for probing the resistivity and the temperature act as strong heat sinks and give rise to temperature gradients also. To minimise this effect, the sample under investigation is made as small as practicable.

(ii) Any temperature gradient inside the graphite furnace gives rise to a thermo emf in the sample and this thermo emf rides over the true voltage output of the sample. Again smaller sample size and placement of the voltage leads very near to each other improves the situation. Further, this problem is circumvented by reversing the current and taking the average value of the voltage output. Alternatively, the thermo emf part is subtracted from the observed value by noting the voltage at zero current through the sample. Moreover, we restricted our data collection by rejecting all data with thermo emf value greater than 0·1% of the voltage output since this indicated sample ends at very different temperatures.

(iii) The electrical resistivity of graphite changes abruptly at about 500°C— due to

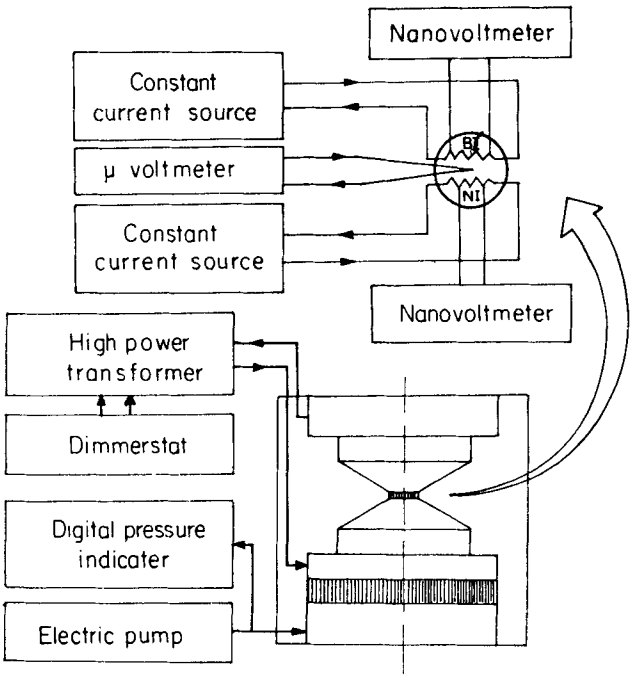

Figure 1. The experimental set-up. Electrically driven hydraulic pump is used to generate the load in the hydraulic press and the oil pressure read by a digital pressure indicator. A high power transformer controlled by the dimmerstat is used to power the graphite furnace, used as internal heater to the sample under investigation.

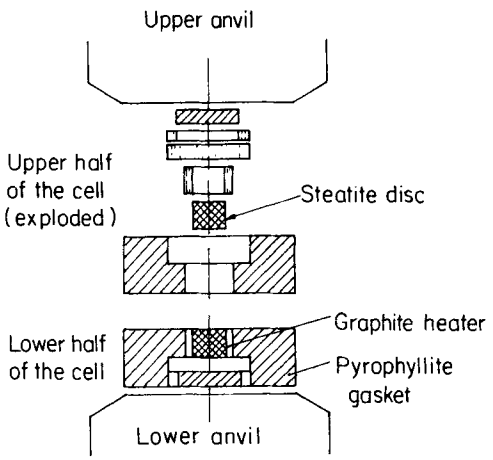

Figure 2. High pressure-high temperature cell assembly. The assembly, as can be seen consists of two symmetrical parts where pyrophyllite has been used in split gasket configuration. Current path is established through anvil → graphite ring → disc → ring → anvil. Pyrophyllite is used to contain the pressure. Silver chloride is used as pressure transmitting medium.

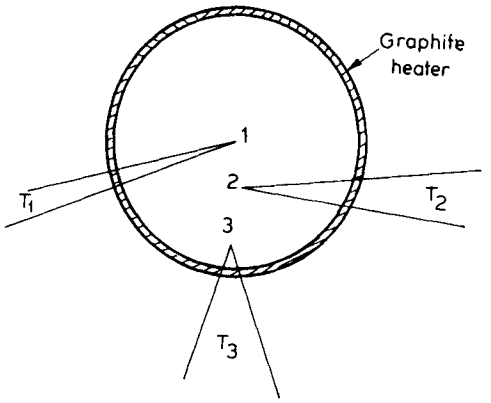

Figure 3. Three thermocouples distributed inside the graphite furnace to check the temperature gradient inside the experimental region. We find that the difference in temperature between the thermocouples at the centre and at the extreme end is less than 5°C in the steady state.

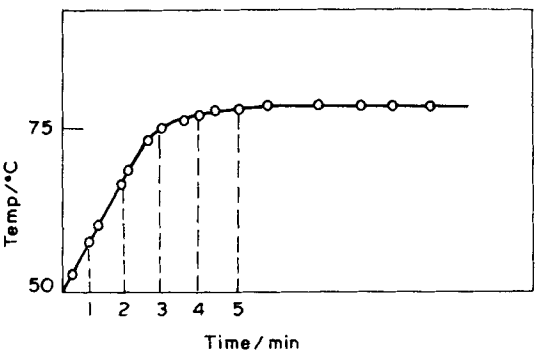

Figure 4. Temperature rise for a sharp power increment to the cell. It is noted that the steady state is achieved within 5 min.

certain physical changes (Shobert 1964; Mrozowski 1952) causing sudden decrease in the cell temperature. To overcome this, the cell was initially raised to 550°C, held there for an hour and then slowly cooled to room temperature. Such a heat treatment resulted in a smoother variation in the electrical resistance of graphite.

(iv) Electrical leads used to probe the voltage output from the sample and the calibrant have to pass through the graphite heater. When the sample circuit is shorted through a graphite heater, it leads to an a.c. (1/10 Hz) signal of small magnitude riding over the true d.c. voltage output from the sample. In order to avoid this difficulty, the graphite heater is cut into four pieces—two big and two small. The small pieces are about 5 % of the bigger ones. The two small graphite pieces are replaced with two similar pyrophyllite pieces. This arrangement is depicted in figure 5. Electrical leads pass through the pyrophyllite pieces, thus insulating the graphite from the sample. This arrangement solves the short circuiting problem, but causes assymetry in the graphite furnace. The temperature gradient and time required to reach the steady state is enhanced. Smaller sample kept at the centre of the cell is used to avoid this problem.

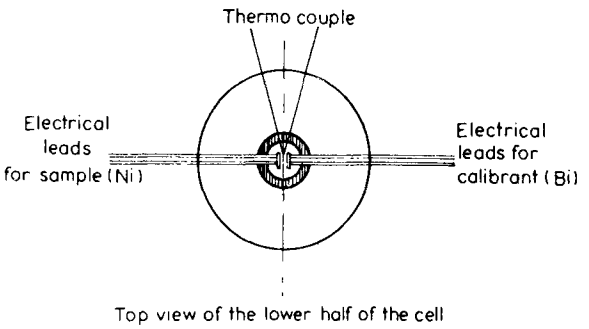

Figure 5. Arrangement showing the placement of the sample (with 4-probes), calibrant (with 4-probes) and the thermocouple to monitor the temperature very near the sample and the calibrant.

3. Pressure emf and thermal pressure

A thermocouple is used to measure the temperature of the internally heated cell. Absolute accuracy of the thermocouple reading depends upon the effect of pressure on the thermal emf. Bundy (1961) has done extensive work in this direction. We shall be referring to the effect of pressure on the thermal emf of Pt/Pt-10% Rh thermocouple used in our experiment. His results indicate that for isothermal environment, pressure has no effect on the thermal emf. However, when a temperature gradient exists, it shows up. In fact for a ΔT of 100°C between the face and the centre, the effect is equivalent to a decrease of 1°C/kbar. In our experiment, the temperature gradient is $\sim$ 5°C in 2 mm. This leads to a correction of less than +0·1°C/kbar to be added to the read value. This also indicates that in our cell, for a pressure of 100 kbar, maximum decrease in the thermal emf will be less than −10°C.

Now we consider the other aspect, that is, the effect of temperature on the sample pressure. Bundy (1964) found an increase of about 16 kbar pressure in the belt apparatus from an initial pressure of 100 kbar when the temperature was raised from room temperature to 500°C. Millet (1968) proposed that pressure might even decrease due to the reduction in the coefficient of friction between the gasket and the anvil face.

Our experiments point to the fact that at least up to 400°C, a thermal pressure of about 1 kbar/100°C is developed. KNO_2 has a phase transition at 6 kbar (Lees 1964) and this is used as a sleeve to bismuth in our cell. A constancy in bismuth output voltage for a continuous increase in the applied load indicates that KNO_2 undergoes a phase transition. Now, at this pressure (6 kbar) when the temperature is raised, bismuth is expected to have a solid liquid transition at 255°C. Instead, we observed melting at 245°C itself. According to the bismuth phase diagram (Cannon 1974), shown in figure 6, this means that the cell pressure is 8·5 kbar.

In a review article, Dekker *et al* (1972) discussed this aspect in detail. Our data agrees well with their observations. For example, Bi I–II transition takes place at 25 kbar. The I + II mixture is obtained by stopping the loading just when the I–II transition initiates. This mixture is heated to obtain pure II phase. If there is no thermal pressure build up, II–L is expected at 180°C. Interestingly enough, heating leads to I–II, II–III, III–IV and IV–L transitions. Melting is observed at 215°C corresponding to a pressure of 28 kbar. Beyond 600°C, dehydration in pyrophyllite takes place. Therefore the estimation of the

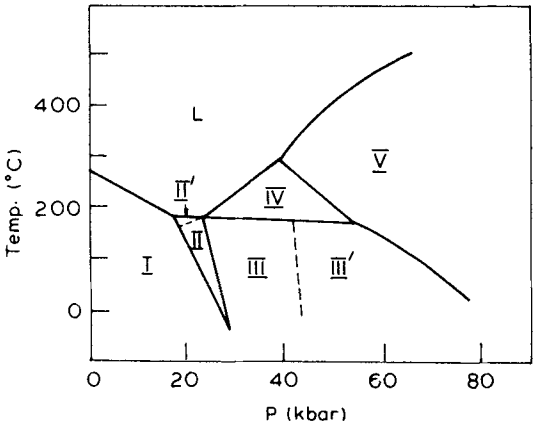

Figure 6. Bismuth phase diagram. At least 8 polymorphic phases can be visualized under hp-ht. Up to 15 kbar, T_m decreases with pressure and beyond it up to 26 kbar, it is almost constant. Beyond 26 kbar $\partial T_m/\partial P$ is positive, characteristic of any normal metal.

thermal pressure becomes somewhat difficult. We are currently performing experiments to evaluate thermal pressure in our hp-ht cell, by following the α–γ Fe phase line (Clougherty and Kaufman 1963).

4. Performance of the hp-ht cell

The cell shown in figure 2 and used in the configuration depicted in figure 1 was tested up to 100 kbar and 1000°C. Pressure calibration is done by following the electrical resistivity of bismuth shown in figure 7. The resistivity changes reflect the transitions I–II (25·4 kbar), II–III (27 kbar) and III–IV (77 kbar) in bismuth. These are indicated by the arrows in the forward direction. On decreasing the pressure a marked hysteresis is observed. Figure 8 indicates our measurements performed at 120°C. The behaviour is in accordance with the bismuth phase diagram (Cannon 1974). The data have been corrected for the thermal pressure increase (1 kbar/100°C). It is noted from figure 8 that the hysteresis is no longer prominent, which would be concommitant with lesser friction in the set-up (Vereschchagin *et al* 1974).

A calibration curve for the input power *vs* the cell temperature as measured by Pt/Pt-10% Rh thermocouple is indicated in figure 9. The cell temperature varied linearly with the input power to the furnace. At 1000°C, the power required is about 1·2 kW. This is definitely higher compared to the power requirement in the belt apparatus (Hall 1956, 1960). Probably this is because of the larger amount of heat conduction through the opposed anvils used as the electrodes.

5. Press calibration

Figure 10 indicates the load *vs* pressure experiments performed at various temperatures by using bismuth as the pressure calibrant. The main point to be noted is that for a given load, the increase in temperature leads to a rise in the internal pressure of the cell. The

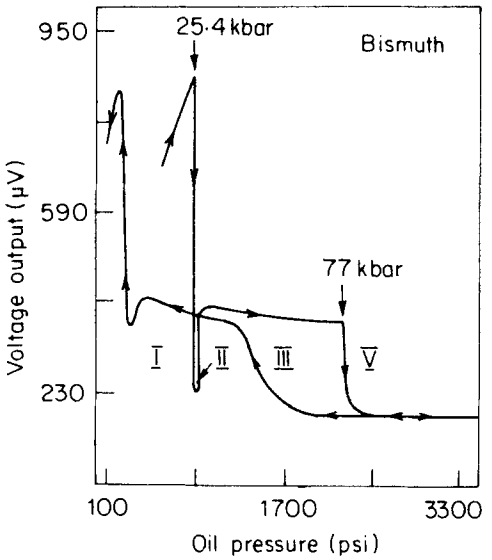

Figure 7. Electrical resistivity data obtained on Bi at room temperature. 25·4 kbar (I–II), 27 kbar (II–III), and 77 kbar (III–IV) can easily be identified. Hysteresis is remarkable.

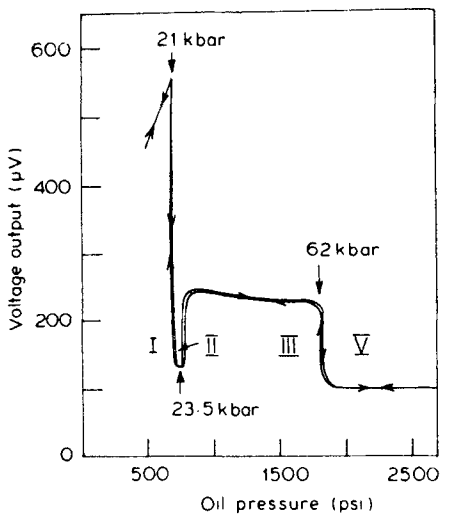

Figure 8. Electrical resistivity data of Bi under high pressure and at a temperature of 120°C. The return cycle indicate that hysteresis is very small at this temperature.

full triangles are the data taken at room temperature. The change is almost linear for all practical purposes. The full circles are the data taken at 120°C. It is interesting to note that even in this case the linear change in pressure with the varying load is obtained. However, the whole curve is shifted up. The data represented by the full squares was obtained by putting two calibrants, namely, Sb and Fe inside the cell. In Sb, II–L transition occurs at 33 kbar and 600°C. In Fe, α–γ transition takes place at 64 kbar and

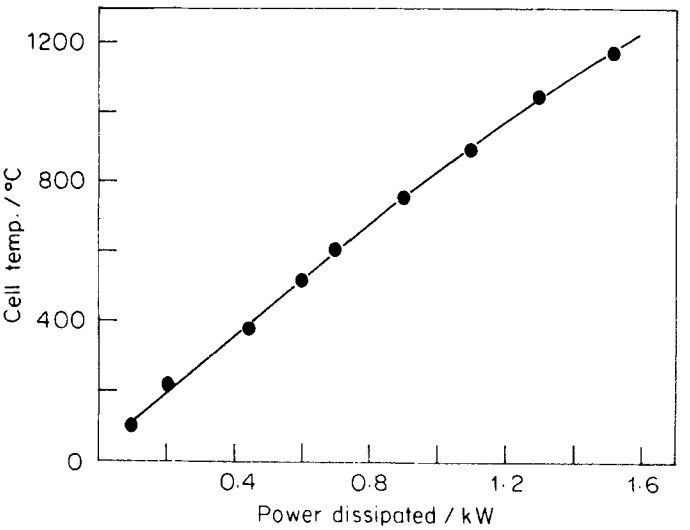

Figure 9. Power input *vs* temperature data. The plot is observed to be linear up to 600°C, beyond which a decrease in slope can be seen.

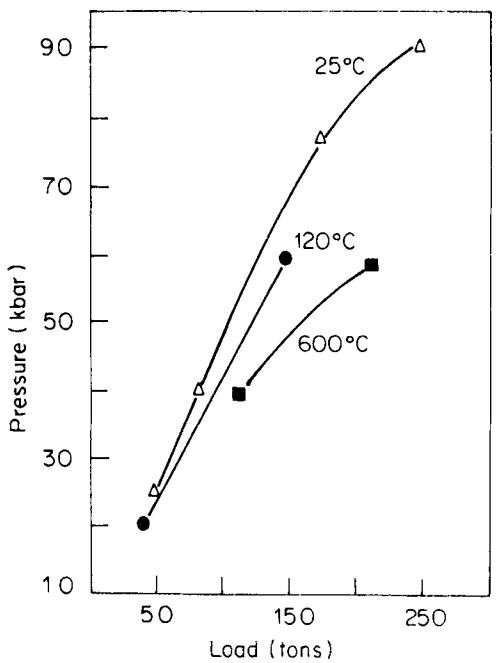

Figure 10. Press calibration curve. It is seen that the slope of the load *vs* pressure curve decreases slowly with temperature. At the moment, it is incomplete.

600°C. The data indicates that the pressure rise with load is not strictly linear, rather the increase is slower. We feel that this is due to the anvil material softening and also due to the decrease in the coefficient of friction in the gasket material (Nishikawa and Akimoto 1971; Millet 1968; Govinda Rajan *et al* 1981). Further work in this direction is under progress.

6. High pressure-high temperature studies on bismuth

99·999% pure bismuth (M/s Hoboken, Belgium) was used in our studies. Resistance data was collected using a nanovoltmeter with the resolution of 10 nV in 10 mV full scale. This leads to a detectability of 1 in 10^4. Experiments were performed at fixed pressure and temperature varied. This was done to minimise the electrical leads snapping and other practical problems.

Figure 11 represents the electrical resistivity measurements on bismuth performed at various fixed pressures and varying temperatures. The full circles represent the data taken at 7 kbar. Initially, it shows a linear rise in resistivity, then undergoes a sudden fall at about 270°C. The full triangles represent data at 22·8 kbar which clearly shows the I–II (70°C), II–III (170°C), III–IV (200°C) and IV–L (240°C) transitions. The open circles represent data obtained at 50 kbar. The initial phase is III and III–IV transition occurs at 200°C, marked by a resistivity minimum. It is worth pointing that our data compares exactly with that of Bundy (1958). In passing we mention that (i) at 7 kbar and 125°C, we observe a break in the resistance behaviour which tallies with the data by Bundy the origin of which is not known. (ii) our consistent efforts to locate I–II′–L have not been successful.

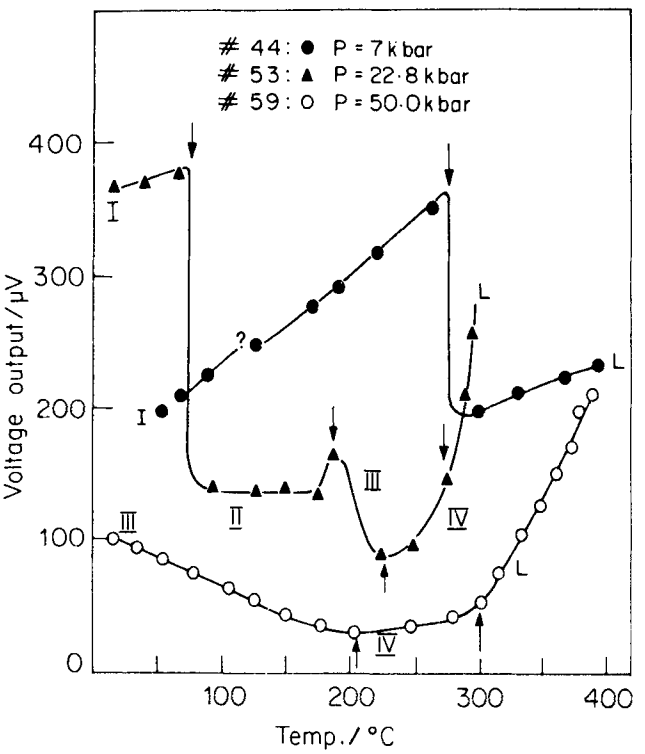

Figure 11. Electrical resistivity data on Bi under high pressure and high temperature. (●) indicate that at 7 kbar, Bi melts at 270°C. At 22·8 kbar, (▲) indicate I $\xrightarrow{70°C}$ II $\xrightarrow{170°C}$ III $\xrightarrow{220°C}$ IV $\xrightarrow{270°C}$ L. At 50 kbar, (○) indicate III $\xrightarrow{200°C}$ IV $\xrightarrow{300°C}$ L.

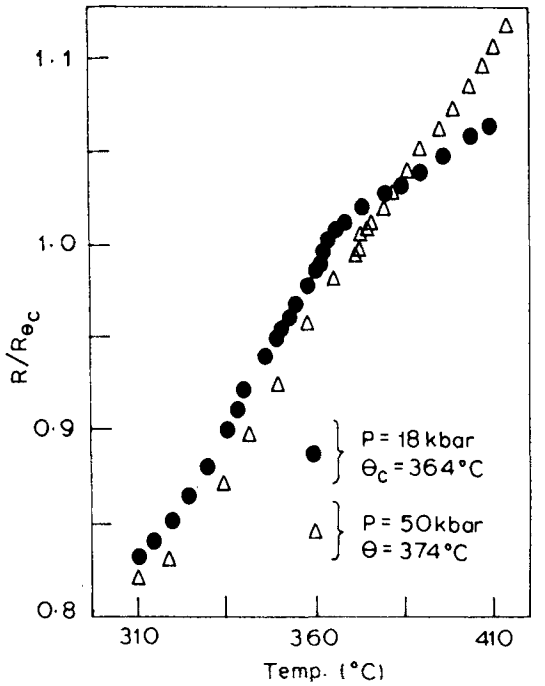

Figure 12. High pressure-high temperature electrical resistivity data on Ni as a test problem. T_c increases with pressure. Also the temperature coefficient of electrical resistivity increases with pressure for temperatures beyond T_c.

7. High pressure-high temperature studies on nickel

High pressure-high temperature electrical resistivity experiments are few in literature. Such measurements are useful for they may be expected to throw some light on the electronic conduction mechanisms in metals and semiconductors. In transition metals, particularly, the resistance studies at high pressures and high temperatures can give information on *s–d* scattering mechanisms at the Fermi level. As a test problem, Ni was chosen and the results obtained are shown in figure 12 to indicate the quality of data obtained with the present cell. Only the temperature range between 300°C and 410°C is shown in the figure to reveal the shift in the Curie temperature of Ni with pressure and the cross-over at the Curie point of the electrical resistivity curve at higher pressures. The interpretation of the results on Ni will form the subject matter of a separate paper.

8. Conclusion

(i) We have developed a hp-ht cell for 4-probe electrical resistivity measurement, with *in situ* pressure and temperature calibration.
(ii) We have used silver chloride as a pressure transmitting medium for achieving quasi-hydrostatic pressure.

(iii) Characterisation of the hp-ht cell has been done following the phase diagram of bismuth.
(iv) Nickel was chosen as a test problem and we have measured the electrical resistivity at high pressures and high temperatures.

Acknowledgements

The authors are thankful to Dr G Venkataraman for his continuous support. They express their indebtness to Prof. E S Raja Gopal of IISc, Bangalore for stimulating discussions. The authors express their appreciation to the referees for their valuable comments.

References

Bovenkerk H P, Bundy H P, Hall H T, Strong H M and Wentorf R H 1959 *Nature (London)* **184** 1094
Bundy F P 1958 *Phys. Rev.* **110** 314
Bundy F P 1961 *Progress in very high pressure research* (eds) F P Bundy, W R Hibbard Jr and H M Strong (New York: John Wiley) 256
Bundy F P 1962 *Science* **137** 1057
Bundy F P 1964 *J. Chem. Phys.* **41** 3809
Cannon John F 1974 *J. Phys. Chem. Ref. Data* **3** 801
Clougherty E V and Kaufman L 1963 *High pressure measurement* (eds) A A Giardini and E C Lloyd (Washington: Butterworths) 152
Coes L L Jr 1953 *Science* **118** 131
Daniels W B and Jones M T 1961 *Rev. Sci. Instrum.* **32** 885
Dekker D L, Bassett W A, Merrill L, Hall H T and Barnett J 1972 *J. Phys. Chem. Ref. Data* **1** 827
Govinda Rajan K, Sastry V S and Rita Khanna 1981 *Rev. Sci. Instrum.* **52** 1734
Hall H T 1956 *J. Phys. Chem.* **59** 1144
Hall H T 1958 *Rev. Sci. Instrum.* **29** 267
Hall H T 1960 *Rev. Sci. Instrum.* **31** 125
Hall H T, Barnett J D and Merrill L 1963 *Science* **139** 111
Lees J 1964 *Advances in high pressure research* (ed.) R S Bradely (New York: Plenum Press) Vol. I 1
Millett L E 1968 Ph.D. Thesis, Brigham Young University, Provo, Utah
Mohammad Yousuf and Govinda Rajan K 1982 *Pramana* **18** 1
Mrozowski S 1952 *Phys. Rev.* **86** 1056
Nishikawa M and Akimoto S 1971 *High Temp. High Pressures* **3** 161
Ringwood A E and Major A 1968 *Phys. Earth Planet. Inter.* **1** 164
Shobert E I II 1964 *Modern materials* (eds) B W Ganser and H H Hansner (New York: Academic Press) Vol. 4 40
Vereshchagin L F, Zubova E V, Stupnikov V A and Aparnikov G L 1974 *High Temp. High Pressure* **6** 509
Wentorf R H Jr. 1957 *J. Chem. Phys.* **26** 956